Electronic Research Archive

ERA, 31(4): 2286–2314.
DOI: 10.3934/era.2023117
Received: 18 December 2022
Revised: 04 February 2023
Accepted: 12 February 2023
Published: 24 February 2023

http://www.aimspress.com/journal/ERA

Research article

Evaluation of nanostructured electrode materials for high-performance supercapacitors using multiple-criteria decision-making approach

Ibrahim M. Hezam[1,*], Aref M. Al-Syadi[2,3], Abdelaziz Foul[1], Ahmad Alshamrani[1] and Jeonghwan Gwak[4,5,6,7]

[1] Department of Statistics & Operations Research, College of Sciences, King Saud University, Riyadh, Saudi Arabia
[2] Department of Physics, Najran University, Najran, Saudi Arabia
[3] Promising Centre for Sensors and Electronic Devices (PCSED), Advanced Materials and Nano-Research Centre, Najran University, Najran, Saudi Arabia
[4] Department of Software, Korea National University of Transportation, Chungju 27469, Korea
[5] Department of Biomedical Engineering, Korea National University of Transportation, Chungju 27469, Korea
[6] Department of AI Robotics Engineering, Korea National University of Transportation, Chungju 27469, Korea
[7] Department of IT & Energy Convergence (BK21 FOUR), Korea National University of Transportation, Chungju 27469, Korea

* **Correspondence:** Email: ialmishnanah@ksu.edu.sa.

Abstract: The enhancement of electrode materials' properties for improving mercantile supercapacitors' performances is a remarkable research area. Throughout recent years, a significant amount of research has been devoted to improving the electrochemical performance of supercapacitors via the improvement of novel electrode materials. The nanocomposite structure provides a greater specific surface area (SSA) and lower ion/electron diffusion tracks, consequently enhancing supercapacitors' energy density and specific capacitance. These significant properties offer a wide range of potential for the electrode materials to be applied in diverse applications. For instance, their applications are in portable electronic systems such as all-solid-state supercapacitors, flexible/transparent supercapacitors and hybrid supercapacitors. The authors of this paper introduced a multi-criteria model to assess the priority of nanostructured electrode materials (NEMs) for high-performance supercapacitors (HPSCs). This work combines Analytic Hierarchy Process (AHP) with the Evaluation Based on Distance from Average

Solution (EDAS) and Grey Relational Analysis (GRA) methods. Herein, the rough concept addresses the uncertainties resulting from the group decision-making process and the vague values of the properties of the NEMs. The modified R-AHP method was employed to find the criteria weights based on the multi-experts' opinions. The results reveal that specific capacitance (SC) and energy density (ED) are the most important criteria. R-AHP was integrated with R-EDAS and R-GRA models to evaluate the fourteen NEMs. The results of the R-EDAS method were compared with those provided by the R-GRA method. The results of the proposed integrated approach confirmed that it results in reliable and reputable ranks that will provide a framework for further applications and help physicists find optimal materials by evaluating various alternatives.

Keywords: high-performance supercapacitors; MCDM; nanostructured electrode materials; rough set

1. Introduction

The conservation of energy and the environment from rapid impairment and the exhaustion of fossil fuels have become issues of concern in recent times. Hence, all are working to solve these problems, including developing clean and alternative energy devices and more developed energy storage/conversion systems. Researchers' efforts have typically centered on two kinds of electrochemical sources: batteries and supercapacitors [1]. High-performance supercapacitors (HPSCs) have attracted much attention in recent years due to their superior power density, long lifecycle, reversibility and few environmental influences [2,3]. Supercapacitors are extensively utilized in some consumer electronics, manufacturing power/energy management and hybrid vehicles.

Nevertheless, the difficulties of low energy density and extraordinary manufacturing costs for electrochemical capacitors (ECs) have been specified as the main challenges in the field of capacitive storage. Supercapacitors should be improved with superior energy density without losing the power density and life cycle [1] to meet the energy requests for many applications. Supercapacitors can be classified into two basic kinds depending on their charge storage method. The electric double-layer capacitance (EDLC) kind produces capacitance from charge segregation at the electrolyte/electrode interface, while the pseudocapacitance kind produces capacitance from rapid faradic responses in the electrode [3–5]. The election of electrode materials and their production plays a critical role in improving the capacitive properties of supercapacitors. Supercapacitors' electrodes should afford thermal stability, corrosion opposition, high electrical conductivity, high SSA, suitable chemical stability and appropriate surface wettability [6]. They must also be relatively low cost and environmentally friendly. In reality, the specific capacitance feature is not only influenced by specific surface area (SSA) but also other essential factors that relate simply to morphology, including pore form, pore size, pore size dispension, and their availability for the electrolyte [7,8].

Moreover, the appropriate size dispensation can enhance the retention capability, which is significant for high power density in supercapacitors' devices. The efficacious dispensation of micro/nanopores in electrode materials can afford rapid mass and ion transference over a continuous track, consequently improving the availability of the electrolyte and making the materials suitable selections for HPSC applications [9]. The quality of supercapacitors relies on the electrode materials as well as their chemical and physical characteristics. In turn, this leads to the diverse employment of supercapacitors and makes some supercapacitors better than others for some particular

applications. Lately, many various supercapacitors have been manufactured in categories relying on electrode materials such as carbon-based materials, transition metal oxides/hydroxides-based materials, conducting polymer-based materials and composite-based materials, as well as the diversity of nanostructured electrode materials (NEMs) for supercapacitors in each category. The variance in the electrochemical characteristics of each electrode material leads to the variance in their utilizations. This variance makes some electrode materials better than others for use in supercapacitors.

Evaluation of NEMs for HPSCs has become an urgent issue for stakeholders so that their goals can be optimally achieved. One of the most well-known tools for assessment and classifying alternatives is the MCDM approach. Integrating two MCDM methods has recently been the strong trend to get the best results in uncertain environments. The uncertainty comes from assumptions, subjective evaluation of the experts, vague data, approximation of the values of the properties, etc. Hence, rough set theory was used in this work to deal with the uncertainty and make the interval boundary flexible, giving the DM flexible judgment, minimizing the information lost and achieving accurate results.

The motivation of this work is that there is no study in the literature addressing the MCDM approach in the assessment ranking of the NEMs for HPSCs based on the authors' knowledge. Additionally, is it possible to select the best NEMs that meet all the criteria and have good properties under an uncertain environment that allows experts to give flexible judgments?

Moreover, all properties of the NEMs for HPSCs are within ranges, which was a motivation to use the rough set concept to deal with these ranges. Another reason for using the rough set concept came from the perspective of the practical application when we collected the data. We know that a property can be approximated by the lower and upper approximations, which motivated us to use the rough set concept for dealing with these ranges.

So, we can briefly summarize the contributions of this work as follows:

- Describing the importance of criteria properties using the linguistic variables given by a group of experts.
- Improving AHP by rough set theory to determine the weights of the criteria.
- Evaluating and ranking the NEMs for HPSCs using the integrated R-AHP with R-EDAS and R-GRA methods.
- Analysis of the comparison results of both R-EDAS and R-GRA methods.

The rest of this article is organized like this: Section 2 presents the criteria and the NEMs for HPSCs. Section 3 introduces the brief of the rough AHP, R-EDAS, R-GRA and the proposed methodology. Section 4 summarizes the results with analysis. Finally, Section 5 gives the conclusion and some points for future works.

2. Criteria and the NEMs for HPSCs

For this section, we identified six criteria and fourteen NEMs for HPSCs. These criteria include the most significant electrochemical characteristics of HPSCs.

2.1. Criteria

The following main criteria were utilized to compare the different NEMs for HPSCs.

1) Specific capacitance (SC):

A supercapacitor consists of two electrodes and an electrolyte between these two electrodes. Because the electrodes can be polarized via a voltage, the ions in the electrolyte make electric double layers of inverse polarity for the electrode's polarity. This means the negative polarized electrodes would have a positive layer of ions at the electrolyte/electrode limit joined by a layer of negative ions in the positive layer to the equilibrium of charges. The opposite is correct for the positively polarized electrodes. In addition, numerous ions can transfer into the double layer to be absorbing ions and collaborate with the pseudocapacitance of the supercapacitor, which relies on surface shape and electrode material. Thus, the specific capacitance (SC) is the amount of charge that can be stored in an energy storage system per unit mass from the electrode [10]. The SC is a very significant criterion to evaluate the performance of the electrode materials for energy storage applications (supercapacitor and battery devices). So, the electrochemical performance is superior when the SC is great.

2) Potential window (PW):

To improve asymmetric supercapacitors, one can take advantage of the difference between the voltages on the two electrodes (negative electrode and positive electrode) to enlarge the working voltage in the electrochemical system. If the electrodes are symmetrical, the electrochemical performance of the supercapacitor will be developed. Otherwise, the electrochemical performance of the energy storage system may be reduced, or the energy storage system may be disrupted [1]. Thus, the widening of the PW leads to improving the performance of the energy storage systems (supercapacitors and batteries).

3) Energy density (ED):

There are two types of energy density: mass-energy density, and volume-energy density. In this work, we will focus on mass-energy density. The mass-energy density of the energy storage systems (supercapacitors and batteries) denotes the capacity of the energy storage system to store the energy for a very long time for its unit mass [11]. So, the ED determines how long the energy storage system can be employed [6]. The ED is a very significant criterion for evaluating the performance of electrode materials for energy storage devices (supercapacitors and batteries). Consequently, the performance of the supercapacitor increases with increasing ED.

4) Power density (PD):

The PD refers to the discharge power volume per unit mass, and it denotes how speedily a device can transfer an amount of energy [6]. The PD is a very significant criterion for assessing the performance of energy storage devices (supercapacitors and batteries).

5) Capacitance retention (CR):

Selecting an exemplary lifetime as an essential parameter for the energy storage systems is extremely related to the kind of device. Choosing favorable materials for electrolytes and electrodes is important, as it affects the cycle stability. Cycle stability, including CR and cycle number (CN), can be estimated by galvanostatic charge/discharge procedures by reiterating the cycles constantly at a fixed current density [12]. The enhancing performance of energy storage devices is determined by their outstanding cycle stability, including superb CR and high CN. For example, the death factor of an energy storage system (battery and supercapacitor) for energy applications is known as 80% of its beginning capacity [13]. The CR for energy storage systems is calculated as the percentage between the initial SC to the SC that is saved after a certain number of cycles. Cyclic stability is an important criterion for estimating the electrochemical performance of energy storage devices. Thus,

the cyclic stability is high when the CR is high.

6) Cycles number (CN):

The CN is defined as the number of full charge-discharge processes before the capacitance of the energy storage devices decreases to under 80% of the start-of-lifetime value [14,15]. So, when the cycle number value rises, the performance of the energy storage device is superior.

2.2. Nanostructured electrode materials (NEMs) for high-performance supercapacitors (HPSCs)

The main kinds of NEMs for HPSCs are the following:

Nanostructured carbon-based materials: activated carbon materials (ACs), carbon nanotubes (CNTs) and graphene.

Transition metal oxides/hydroxides-based materials: ruthenium oxide (RuO_2), manganese dioxide (MnO_2), nickel oxide (NiO), nickel hydroxide ($Ni(OH)_2$) and vanadium pentoxide (V_2O_5).

Conducting polymer-based material: polyaniline (PANI) and polypyrrole (PPy).

Nanocomposite-based materials: carbon-carbon composites (C-C), carbon- metal oxides composites (C-MOs), carbon- conducting polymers composites (C-CPs) and metal oxides- conducting polymers composites (MOs-CPs).

1) Activated carbon materials (ACs)

ACs are the most generally utilized materials for EDLC electrodes with medium cost [10] that show a complicated porous structure involving micropores (lower than 2 nm), mesopores (between 2 and 50 nm) and macropores greater than 50 nm, leading to possessing a great SSA [11,12]. Moreover, although their electrical conductivity is less than (1250–2500 Sm^{-1}), it is still appropriate for supercapacitors. These properties indicate that ACs are considered beneficial electrode materials for supercapacitors [6]. ACs show that many of the physical and chemical characteristics rely on the carbon precursors utilized and activation procedures that strongly affect the SSA, porous construction and pore size dispensation [13].

2) Carbon nanotubes (CNTs)

CNT electrode materials have been advanced owing to their individual characteristics, such as their attainable exterior construction with great SSA and specified interior network of mesopores, outstanding electrical conductivity, chemical and thermal stability and low mass density. Moreover, the mechanical flexibility of the CNTs and their open lattice afford their linking to active material, superior connection and creating a continued dispensation that produces a high SSA [14]. CNTs would be utilized as electrode materials for supercapacitors in the composite shape over other materials, such as metal oxides (MOs), graphene and polymer [6].

3) Graphene

Graphene consists of a one-atom-thick layered 2D construction with sp2-bonded carbon atoms coordinated in a crystalline honeycomb structure [15,16]. As a distinctive carbon material, graphene has outstanding properties, including excellent morphological and mechanical characteristics, good electrical conductivity, high carrier mobility, high chemical stability and high SSA [6]. Moreover, the 2D construction of graphene reduces the thickness of the electrode, which yields a higher voltage window, larger flexibility and thermal and chemical stability [16]. So, graphene is a strong candidate for energy storage systems owing to its features [15]. Consequently, graphene would be employed as electrodes in the system of HPSCs. Meanwhile, compared with other carbon-based materials that contain carbon (for instance, ACs and CNTs), graphene-based electrodes do not rely on the regularity of pores in solid

materials [17].

4) Ruthenium oxide (RuO_2)

RuO_2 is one of the most studied transition metal oxides (TMOs) for supercapacitor electrodes owing to its outstanding electrical conductivity, outstanding thermal and chemical stability, wide PW, long life-cycle, extremely reversible redox reaction, great theoretical capacity and excellent rate ability [18]. RuO_2 materials are costly, which reduces their wide-range applications. For developing cost-efficient materials, RuO_2 hybrids were combined with other materials rich in carbon or pseudocapacitance to decrease the quantity of RuO_2 without affecting the efficiency [19]. For example, a nanosized RuO_2/polyaniline (PANI)/carbon dual-shelled blank spheres nanocomposite was patterned over electro-polymerization processes [20].

5) Manganese dioxide (MnO_2)

MnO_2 is utilized as electrodes for supercapacitors owing to its outstanding characteristics such as superior electrochemical performance, low cost and low environmental influence, which make it beneficial for a wide range of applications, such as in biosensors, molecular absorption, energy storage devices, ion interchange and catalysis [21]. MnO_2 has a lower cost and greater obtainability compared with RuO_2-based materials [22]. In addition, other outstanding characteristics, such as a wide-ranging PW, low toxicity and a great SC, make it a favorable electrode alternative [23].

6) Nickel oxide (NiO)

NiO nanomaterial has attracted the attention of researchers as electrodes for supercapacitors owing to the reduced diffusion tracks, rapid redox reactions and a great SSA in the solid phase [24,25]. NiO is a favorable pseudocapacitive electrode material for supercapacitors because of its characteristics, such as great electrochemical capacitance, thermal and chemical stability, simplistic synthesis, sensible cost, profusion and environmental friendliness [26].

7) Nickel hydroxide ($Ni(OH)_2$)

$Ni(OH)_2$ has recently drawn researchers' attention because of its outstanding characteristics, such as its extraordinary theoretical capacity, good rate ability, ready obtainability, lesser cost, environmental friendliness and outstanding chemical and thermal stability [27]. Consequently, α-$Ni(OH)_2$ is the most potent energy storage-type material used in supercapacitor applications; it is utilized as an anode in nickel-based batteries and is also appropriate for HPSCs [28].

8) Vanadium pentoxide (V_2O_5)

V_2O_5 is an inorganic-intercalation compound, and it has drawn the attention of researchers as an appropriate electrode for pseudocapacitors owing to its natural profusion, extraordinary ED, low cost, low toxicity, varied oxidation states (+2 to +5), simplicity of preparation and great electrochemical capacity [29]. V_2O_5 offers a high electrochemical capacity and wide-range voltage window related to the greater oxidation state of V, which works on transporting a high number of electrons [30]. However, low SSA and the low solubility of V_2O_5 decrease the electrochemical capacitance development. Moreover, V_2O_5 is widely suggested as an electrode material for supercapacitors because of its controllable morphology [6].

9) Polyaniline (PANI)

PANI is a popular conducting polymers composites (CPs) electrode material because of its great electrical conductivity, low weight, greater electrochemical capacity, simplistic synthesis and low cost. Moreover, PANI is mechanically elastic and environmentally friendly [31]. Additionally, PANI offers a wide range of electrochromic characteristics, such as showing several colors, owing to its numerous oxidation states and protonation forms. These features make it a fit candidate for the manufacture of

electrochromic HPSCs [32].

10) Polypyrrole (PPy)

The increasing demand for advanced energy storage systems for electrochemical electrode materials could be obtained from conductive polymer hydrogels with mechanical elasticity and adaptable capacitive characteristics. PPy is a conductive polymer that draws the attention of investigators. It has a greater density and superior elasticity compared with other CPs. It could bear a rapid redox reaction for the charge storage and shows a great conductivity value in the range of (10−500 S cm^{-1}) [33].

11) Carbon-carbon composites (C-C)

The great SC of the carbon materials emerges from the efficient SSA, which can increase the connection between the electrode and electrolyte. Consequently, enhancing the high SSA of these composites produces increasingly higher energy and PD in supercapacitors. There are numerous kinds of carbon materials that could be utilized to construct carbon-based composites [6].

12) Carbon-metal oxides composites (C-MOs)

TMOs possess low SC, low electrical conductivity and poor chemical stability. The nanocomposites made from mixing TMOs and carbon compounds could enhance the electrochemical characteristics of supercapacitors. Consequently, in adding the MOs, there are diverse compositions of MOs and carbon-based composites, which have demonstrated greater SSA than those of pure MOs and carbon composites [34].

13) Carbon-conducting polymers composites (C-CPs)

There are various carbon composites that are mixed with CPs to create nanocomposites. For example, the nanocomposite utilizing the CPs as an anode and the carbon as a cathode could afford greater energy and PD than EDLCs and improved cycling characteristics compared with pseudocapacitors [35].

14) Metal oxides-conducting polymers composites (MOs-CPs)

The MOs/CPs-based composites are other substitution compositions for electrode materials that afford improved electrochemical characteristics in supercapacitors resulting from combining the MOs and CPs [36]. The rate ability, SC and cycling stability could be improved compared with pure MOs and pure CPs composite for electrode materials by improving the compositions of MOs mixed with CPs yielding electrode with enhanced electrical conductivity [6].

3. Proposed methodology

This section consists of three subsections, where the first subsection addresses the rough concept and the AHP method, the second subsection introduces the rough EDAS method, and the third subsection presents the rough GRA method. Also, the proposed methodology is summarized in the last section.

3.1. Rough AHP

The analytic hierarchy process (AHP) [37] method is one of the MCDM methods widely used to solve many complicated decision-making problems. On the other hand, it has become necessary to deal with vague information. That is why many mathematical concepts were proposed to handle the imprecise data, like the integrated AHP method with the fuzzy set, gray, rough, Fermatean fuzzy, neutrosophic, etc. for determining the criteria weights based on the experts' opinions regarding

handling the subjectivity and the vague information.

In this work, the AHP method will be used to calculate the weights of the evaluation criteria with the help of rough numbers.

A rough set (Pawlak [38]) is one of the mathematical tools that can eliminate the vagueness and find hidden data using the upper and lower approximation values.

Let us suppose a set of n classes of ideas, $\mathcal{R}(x_1, x_2, \dots, x_n)$ where $x_1 < x_2 < \cdots < x_n$.

Let us take $\mathcal{Y}$ as an arbitrary object of $\mathcal{U}$. Then, the lower and upper approximation of x_i can be defined respectively as follows:

Lower approximation $\underline{Apr}(x_i) = \mathcal{U}\{\mathcal{Y} \in \mathcal{U}/\mathcal{R}(\mathcal{Y}) \leq x_i\}$ and upper approximation $\overline{Apr}(x_i) = \mathcal{U}\{\mathcal{Y} \in \mathcal{U}/\mathcal{R}(\mathcal{Y}) \geq x_i\}$. Also, we can define the boundary region as follows:

Boundary region $\mathcal{BR} = \mathcal{U}\{\mathcal{Y} \in \mathcal{U}/\mathcal{R}(\mathcal{Y}) \neq x_i\} = \mathcal{U}\{\mathcal{Y} \in \mathcal{U}/\mathcal{R}(\mathcal{Y}) < x_i\} \cup \mathcal{U}\{\mathcal{Y} \in \mathcal{U}/\mathcal{R}(\mathcal{Y}) > x_i\}$.

Hence, we can represent the x_i by a rough number, where the boundary of the interval can be defined as follows:

Rough number: $\mathcal{RN} = \left[\left(\underline{Lim}(x_i)\right), \left(\overline{Lim}(x_i)\right)\right]$,

Interval of boundary region $\mathcal{IBR} = \left(\overline{Lim}(x_i)\right) - \left(\underline{Lim}(x_i)\right)$

We can normalize the rough number $\mathcal{RN}(a_i)$ using Eq (1) as

$$\mathcal{RN}(x_i) = \left[\left(\underline{Lim}(x_i)\right), \left(\overline{Lim}(x_i)\right)\right] = \begin{cases} \underline{Lim}(x_i) = \frac{\underline{Lim}(x_i) - \min_i\{\underline{Lim}(x_i)\}}{\max_i\{\overline{Lim}(x_i)\} - \min_i\{\underline{Lim}(x_i)\}} \\ \overline{Lim}(x_i) = \frac{\overline{Lim}(x_i) - \min_i\{\underline{Lim}(x_i)\}}{\max_i\{\overline{Lim}(x_i)\} - \min_i\{\underline{Lim}(x_i)\}} \end{cases} \tag{1}$$

Also, Eq (2) is used to calculate the crisp value.

$$CN_i^{crisp} = \min_i\{\underline{Lim}(x_i)\} + \beta_i \cdot \left[\max_i\{\overline{Lim}(x_i)\} - \min_i\{\underline{Lim}(x_i)\}\right] \tag{2}$$

where

$$\beta_i = \frac{\underline{Lim}(x_i) \cdot \left(1 - \underline{Lim}(x_i)\right) + \overline{Lim}(x_i) \cdot \overline{Lim}(x_i)}{1 - \underline{Lim}(x_i) + \overline{Lim}(x_i)} \tag{3}$$

Now, the rough set will be combined with the AHP method to be an effective assessment framework to deal with alternatives based on the related multiple criteria. The main procedures of the R-AHP are presented as follows:

Step 1: Build the pairwise comparison matrix $\mathcal{A}^e$ for each e^{th} expert and test the consistency.

$$\mathcal{A}^e = \begin{bmatrix} 1 & a_{12}^e & \dots & a_{1m}^e \\ a_{21}^e & 1 & \dots & a_{2m}^e \\ \vdots & \vdots & \ddots & \vdots \\ a_{m1}^e & a_{m2}^e & \dots & 1 \end{bmatrix} \tag{4}$$

Step 2: Test the consistency ratio ($\mathcal{CR}$) using Eq (5), where the acceptable value of $\mathcal{CR}$ must be less than 0.1. In case the $\mathcal{CR} > 0.1$, the experts are recommended to evaluate the decision matrix for superior consistency.

$$\mathcal{CR} = \frac{\mathcal{CI}}{\mathcal{RI}} \tag{5}$$

where $\mathcal{CI}$ is given as

$$\mathcal{CI} = \frac{\lambda_{max} - n}{n-1} \tag{6}$$

where n is the number of criteria, λ_{max} is the mean of the weighted sum vector on the regarding criteria, and $\mathcal{RI}$ is a random index given in Table .

Table 1. Random index via Saaty [39].

Matrix size	1	2	3	4	5	6	7	8	9	10
$\mathcal{RI}$	0	0	0.58	0.90	1.12	1.24	1.32	1.41	1.45	1.49

Step 3: Construct the group decision matrix.

$$\tilde{\mathcal{A}} = \begin{bmatrix} 1 & \tilde{a}_{12} & \dots & \tilde{a}_{1m} \\ \tilde{a}_{21} & 1 & \dots & \tilde{a}_{2m} \\ \vdots & \vdots & \ddots & \vdots \\ \tilde{a}_{m1} & \tilde{a}_{m2} & \dots & 1 \end{bmatrix} \tag{7}$$

where $\tilde{a}_{ij} = \{a_{ij}^1, a_{ij}^2, \dots, a_{ij}^s\}$

Step 4: Convert the element a_{ij} in group decision matrix $\tilde{\mathcal{A}}$ into rough number as follows:

$$\mathcal{RN}(a_{ij}^e) = [a_{ij}^{e\ell} \quad a_{ij}^{eu}] \tag{8}$$

where $a_{ij}^{e\ell}, a_{ij}^{eu}$ are the lower and upper limits of $\mathcal{RN}(a_{ij})$.

We get a rough sequence $\mathcal{RN}(\tilde{a}_{ij})$ as

$$\mathcal{RN}(\tilde{a}_{ij}) = \{[a_{ij}^{1\ell} \quad a_{ij}^{1u}], [a_{ij}^{2\ell} \quad a_{ij}^{2u}], \dots, [a_{ij}^{s\ell} \quad a_{ij}^{su}]\}. \tag{9}$$

Calculate the average rough interval by

$$\mathcal{R}\overline{\mathcal{N}}(a_{ik}) = [a_{ij}^{\ell} \quad a_{ij}^{u}] \tag{10}$$

where

$$a_{ij}^{\ell} = \frac{a_{ij}^{1\ell} + a_{ij}^{2\ell} + \cdots + a_{ij}^{s\ell}}{s} \tag{11}$$

$$a_{ij}^{u} = \frac{a_{ij}^{1u} + a_{ij}^{2u} + \cdots + a_{ij}^{su}}{s} \tag{12}$$

Step 5: Form the rough group decision matrix $\mathcal{M}$ as

$$\mathcal{M} = \begin{bmatrix} [1\ \ 1] & [a_{12}^{\ell}\ \ a_{12}^{u}] & \ldots & [a_{1m}^{\ell}\ \ a_{1m}^{u}] \\ [a_{21}^{\ell}\ \ a_{21}^{u}] & [1\ \ 1] & \ldots & [a_{2m}^{\ell}\ \ a_{2m}^{u}] \\ \vdots & \vdots & \ddots & \vdots \\ [a_{m1}^{\ell}\ \ a_{m1}^{u}] & [a_{m2}^{\ell}\ \ a_{m2}^{u}] & \ldots & [1\ \ 1] \end{bmatrix} \tag{13}$$

Step 6: Calculate the rough weight w_i and its normalization $\dot{w}_i$ of each criterion by Eqs (14) and (15), respectively:

$$w_i = \left[\sqrt[m]{\prod_{k=1}^{m} a_{ik}^{\ell}},\ \sqrt[m]{\prod_{k=1}^{m} a_{ik}^{u}} \right] \tag{14}$$

$$\dot{w}_i = \frac{w_i}{\max w_i^{u}} \tag{15}$$

Step 7: Obtain the crisp weights using Eqs (1)−(3).

3.2. Rough EDAS method

The evaluation based on distance from average solution (EDAS) (Ghorabaee et al. [40]) is updated to be able to deal with imprecise data based on the rough concept.

In the previous section, the rough AHP is used to calculate the relative importance of each criterion. Herein, rough EDAS is introduced to aggregate individual priorities and evaluate design concept alternatives, and the main steps of the new modified method are as follows:

Step 1: Build the rough group decision matrix $\mathcal{M}$ as

$$\mathcal{M} = \begin{bmatrix} [x_{11}^{\ell}\ \ x_{11}^{u}] & [x_{12}^{\ell}\ \ x_{12}^{u}] & \ldots & [x_{1m}^{\ell}\ \ x_{1m}^{u}] \\ [x_{21}^{\ell}\ \ x_{21}^{u}] & [x_{22}^{\ell}\ \ x_{22}^{u}] & \ldots & [x_{2m}^{\ell}\ \ x_{2m}^{u}] \\ \vdots & \vdots & \ddots & \vdots \\ [x_{n1}^{\ell}\ \ x_{n1}^{u}] & [x_{n2}^{\ell}\ \ x_{n2}^{u}] & \ldots & [x_{nm}^{\ell}\ \ x_{nm}^{u}] \end{bmatrix} \tag{16}$$

Step 2: Find the range of the average $\mathcal{AV}$ for all criteria using Eq (23).

$$\mathcal{AV} = \left[\mathcal{AV}_j^{\ell}\ \ \mathcal{AV}_j^{u} \right]_{1\times m},\ \mathcal{AV}_j^{\ell} = \frac{\sum_{i=1}^{n} x_{ij}^{\ell}}{n},\ \mathcal{AV}_j^{u} = \frac{\sum_{i=1}^{n} x_{ij}^{u}}{n} \tag{17}$$

Step 3: Find the positive and negative distances from average ($\mathcal{PDA}$ and $\mathcal{NDA}$) via Eqs (18) and (19), respectively:

$$\mathcal{PDA} = \left[\mathcal{PDA}_{ij}^{\ell} \;\; \mathcal{PDA}_{ij}^{u}\right] =$$

$$\begin{cases} \left[\frac{\max\left(0,\left(x_{ij}^{\ell}-\mathcal{AV}_{j}^{\ell}\right)\right)}{\mathcal{AV}_{j}^{\ell}}, \;\; \frac{\max\left(0,\left(x_{ij}^{u}-\mathcal{AV}_{j}^{u}\right)\right)}{\mathcal{AV}_{j}^{u}}\right] & if\ the\ j^{th}\ criterion\ is\ beneficial \\ \left[\frac{\max\left(0,\left(\mathcal{AV}_{j}^{\ell}-x_{ij}^{\ell}\right)\right)}{\mathcal{AV}_{j}^{\ell}}, \;\; \frac{\max\left(0,\left(\mathcal{AV}_{j}^{u}-x_{ij}^{u}\right)\right)}{\mathcal{AV}_{j}^{u}}\right] & if\ the\ j^{th}\ criterion\ is\ non-beneficial \end{cases} \tag{18}$$

$$\mathcal{NDA} = \left[\mathcal{NDA}_{ij}^{\ell}, \mathcal{NDA}_{ij}^{u}\right] =$$

$$\begin{cases} \left[\frac{\max\left(0,\left(\mathcal{AV}_{j}^{\ell}-x_{ij}^{\ell}\right)\right)}{\mathcal{AV}_{j}^{\ell}}, \frac{\max\left(0,\left(\mathcal{AV}_{j}^{u}-x_{ij}^{u}\right)\right)}{\mathcal{AV}_{j}^{u}}\right] & if\ the\ j^{th}\ criterion\ is\ beneficial \\ \left[\frac{\max\left(0,\left(x_{ij}^{\ell}-\mathcal{AV}_{j}^{\ell}\right)\right)}{\mathcal{AV}_{j}^{\ell}}, \frac{\max\left(0,\left(x_{ij}^{u}-\mathcal{AV}_{j}^{u}\right)\right)}{\mathcal{AV}_{j}^{u}}\right] & if\ the\ j^{th}\ criterion\ is\ non-beneficial \end{cases} \tag{19}$$

$\mathcal{PDA}_{ij}$ is the positive distance of i^{th} alternative from average solution in terms of j^{th} criterion.

$\mathcal{NDA}_{ij}$ is the negative distance of i^{th} alternative from average solution in terms of j^{th} criterion.

Step 4: Compute the weighted sums of the $\mathcal{PDA}$ and $\mathcal{NDA}$ by Eqs (20) and (21):

$$\left[\mathcal{SP}_{i}^{\ell} \;\; \mathcal{SP}_{i}^{u}\right] = \left[\sum_{j=1}^{m} w_{i}^{\ell} \;\; \mathcal{PDA}_{ij}^{\ell}, \;\; \sum_{j=1}^{m} w_{i}^{u} \;\; \mathcal{PDA}_{ij}^{u}\right] \tag{20}$$

$$\left[\mathcal{SN}_{i}^{\ell} \;\; \mathcal{SN}_{i}^{u}\right] = \left[\sum_{j=1}^{m} w_{i}^{\ell} \;\; \mathcal{NDA}_{ij}^{\ell}, \;\; \sum_{j=1}^{m} w_{i}^{u} \;\; \mathcal{NDA}_{ij}^{u}\right] \tag{21}$$

where w_j is the weight of j^{th} criterion.

Step 5: Normalize the weighted sums via Eqs (22) and (23):

$$\mathcal{NE}_{i}^{\ell} = \frac{1}{2} \times \left(\frac{\mathcal{SP}_{i}^{\ell}}{\max\limits_{i} \mathcal{SP}_{i}^{\ell}} + 1 - \frac{\mathcal{SN}_{i}^{\ell}}{\max\limits_{i} \mathcal{SN}_{i}^{\ell}}\right) \tag{22}$$

$$\mathcal{NE}_{i}^{u} = \frac{1}{2} \times \left(\frac{\mathcal{SP}_{i}^{u}}{\max\limits_{i} \mathcal{SP}_{i}^{u}} + 1 - \frac{\mathcal{SN}_{i}^{u}}{\max\limits_{i} \mathcal{SN}_{i}^{u}}\right) \tag{23}$$

Step 6: Obtain the crisp scores using Eqs (1)−(3).

3.3. Rough GRA

In 1989, Deng [41] proposed a new MCDM method, grey relational analysis (GRA), where the relation degree measures the degree of similarity and difference between two sequences. This subsection combines the rough set with the GRA method to solve the given problem.

Step 1: Build the rough group decision matrix $\mathcal{M}$ as in Eq (16).

Step 2: Calculate the weighted normalized relationship matrix in rough number form as

$$x_{ij}'^{\ell} = \frac{x_{ij}^{\ell}}{max_{j=1}^{m}\left\{\max\left[x_{ij}^{\ell}, x_{ij}^{u}\right]\right\}} \tag{24}$$

$$x_{ij}'^{u} = \frac{x_{ij}^{u}}{max_{j=1}^{m}\left\{\max\left[x_{ij}^{\ell}, x_{ij}^{u}\right]\right\}} \tag{25}$$

Step 3: Calculate the weighted normalized rough relationship matrix as

$$v_{ij}^{\ell} = w_i'^{\ell} \times x_{ij}'^{\ell} \tag{26}$$

$$v_{ij}^{u} = w_i'^{u} \times x_{ij}'^{u} \tag{27}$$

Step 4: Obtain the weighted normalized rough relationship matrix $\mathcal{M}'$ as

$$\mathcal{M}' = \begin{bmatrix} \left[v_{11}^{\ell}\ v_{11}^{u}\right] & \left[v_{12}^{\ell}\ v_{12}^{u}\right] & \cdots & \left[v_{1m}^{\ell}\ v_{1m}^{u}\right] \\ \left[v_{21}^{\ell}\ v_{21}^{u}\right] & \left[v_{22}^{\ell}\ v_{22}^{u}\right] & \cdots & \left[v_{2m}^{\ell}\ v_{2m}^{u}\right] \\ \vdots & \vdots & \ddots & \vdots \\ \left[v_{n1}^{\ell}\ v_{n1}^{u}\right] & \left[v_{n2}^{\ell}\ v_{n2}^{u}\right] & \cdots & \left[v_{nm}^{\ell}\ v_{nm}^{u}\right] \end{bmatrix} \tag{28}$$

Step 5: Compute the ideal reference and the reference sequence using Eqs (29) and (30):

$$v^{0}(i) = \left\{max_{j=1}^{m}\left(v_{ij}^{u}\right)\right\},\ \ i = 1,2,\ldots,n \tag{29}$$

$$\mathcal{V}^{0}(i) = \{v^{0}(1), v^{0}(2), \ldots, v^{0}(n)\} \tag{30}$$

Step 6: Compute the deviation coefficient d_{ij}:

$$d_{ij}^{\ell} = v^{0}(i) - v_{ij}^{\ell}, \quad i = 1,2,\ldots,n; j = 1,2,\ldots,m \tag{31}$$

$$d_{ij}^{u} = v^{0}(i) - v_{ij}^{u}, \quad i = 1,2,\ldots,n; j = 1,2,\ldots,m \tag{32}$$

Step 7: Build the deviation coefficient matrix $\mathcal{D}$:

$$\mathcal{D} = \begin{bmatrix} \left[d_{11}^{\ell}\ d_{11}^{u}\right] & \left[d_{12}^{\ell}\ d_{12}^{u}\right] & \cdots & \left[d_{1m}^{\ell}\ d_{1m}^{u}\right] \\ \left[d_{21}^{\ell}\ d_{21}^{u}\right] & \left[d_{22}^{\ell}\ d_{22}^{u}\right] & \cdots & \left[d_{2m}^{\ell}\ d_{2m}^{u}\right] \\ \vdots & \vdots & \ddots & \vdots \\ \left[d_{n1}^{\ell}\ d_{n1}^{u}\right] & \left[d_{n2}^{\ell}\ d_{n2}^{u}\right] & \cdots & \left[d_{nm}^{\ell}\ d_{nm}^{u}\right] \end{bmatrix} \tag{33}$$

Step 8: Compute the grey relational coefficient as

$$g_{ij}^{\ell} = \frac{min_{i=1}^{m} min_{j=1}^{n}\ d_{ij}^{\ell} + \eta \times max_{i=1}^{m} max_{j=1}^{n}\ d_{ij}^{\ell}}{d_{ij}^{\ell} + \eta \times max_{i=1}^{m} max_{j=1}^{n}\ d_{ij}^{\ell}} \tag{34}$$

$$g_{ij}^{u} = \frac{min_{i=1}^{m} min_{j=1}^{n}\ d_{ij}^{u} + \eta \times max_{i=1}^{m} max_{j=1}^{n}\ d_{ij}^{u}}{d_{ij}^{u} + \eta \times max_{i=1}^{m} max_{j=1}^{n}\ d_{ij}^{u}} \tag{35}$$

where the distinguishing coefficient η is $0 \leq \eta \leq 1$, and for good stability we set $\eta = 0.5$ [42].

Step 9: Compute the grey relational degree as

$$\Gamma_j^{\ell} = \frac{\sum_{i=1}^{m} w_i^{\ell} g_{ij}^{\ell}}{m}, \quad j = 1, \ldots, n \tag{36}$$

$$\Gamma_j^{u} = \frac{\sum_{i=1}^{m} w_i^{u} g_{ij}^{u}}{m}, \quad j = 1, \ldots, n \tag{37}$$

It is probable that when Γ_j is large, it is closer to the ideal reference value and has a higher priority.

Step 10: Calculate the crisp scores using Eqs (1)−(3).

We can summarize the proposed methodology in the following flowchart:

Assessment of the criteria of NEMs for HPSCs
Step 1: Obtain the linguistic evaluations for the criteria of NEM for HPSC from the multi-experts. *Step 2:* Convert the linguistic evaluations to scores. *Step 3:* Calculate the rough assessment.
Determine the range of the criteria weights
Step 4: Use the rough AHP to determine the criteria weights.
NEMs for HPSCs ranking based on rough EDAS and rough GRA methods
Step 5: Use the rough EDAS for ranking the NEMs for HPSCs. *Step 6:* Use the rough GRA for ranking the NEMs for HPSCs. *Step 7:* Perform a comparative analysis and get the correlation and p-value between the obtained ranks. *Step 8:* Recommend the priority of the criteria and the superior of the NEMs for HPSCs.

Figure 1. The flowchart of the proposed approach.

4. Results and discussion

In this section, the two parts will be presented. In the first part, the rough AHP will be used to determine the range of the criteria weights to use later. In the second part, R-EDAS and R-GRA methods will be used to evaluate fourteen NEMs based on the criteria with their weights obtained in the first part.

4.1. The results of the rough-AHP method

First, the linguistic values with their scores were defined for the relative significance of the criteria as listed in Table 2.

Table 2. Linguistic variables in terms of rough set.

Linguistic term	Score
Exactly equal	1
Very low important	2
Low important	3
Middle important	4
High important	5
Very High important	6

Table 3 collects the individual preferences of each expert for each criterion with the help of the linguistic terms and their scores in Table 2.

Table 3. Collecting the multi-experts' opinions.

Three experts		Specific capacitance	Potential window	Energy density	Power density	Stability	
						Capacitance retention	Cycles number
Specific capacitance		-	4, 5, 6	1, 1, 1	2, 2, 2	2, 2, 3	2, 3, 2
Potential window		1/4, 1/5, 1/6	-	1/3, 1/5, 1/6	1/3, 1/4, 1/5	1/2, 1/2, 1/2	1/2, 1/2, 1/2
Energy density		1, 1, 1	3, 5, 6	-	2, 2, 2	2, 2, 3	2, 3, 2
Power density		1/2, 1/2, 1/2	3, 4, 5	1/2, 1/2, 1/2	-	2, 2, 2	2, 2, 2
Stability	Capacitance retention	1/2, 1/2, 1/3	2, 2, 2	1/3, 1/2, 1/2	1/2, 1/2, 1/2	-	1, 1, 2
	Cycles number	1/2, 1/3, 1/2	2, 2, 2	1/2, 1/3, 1/2	1/2, 1/21/, 2	1/2, 1, 1	-

The multi-experts' scores were transformed to the rough interval as presented in Table 4. Let us take {3,4,5} as an example for showing the converting process to interval number.

$$\underline{Lim}(3) = 3, and\ \overline{Lim}(3) = \frac{3+4+5}{3} = 4.$$

$$\underline{Lim}(4) = \frac{3+4}{2} = 3.5, and\ \overline{Lim}(4) = \frac{4+5}{2} = 4.5.$$

$$\underline{Lim}(5) = \frac{3+4+5}{3} = 4, and\ \overline{Lim}(5) = 5.$$

This can be expressed in rough numbers:

$$\mathcal{RN}(3) = \left[\left(\underline{Lim}(3)\right), \left(\overline{Lim}(3)\right)\right] == [3, 4]$$

$$\mathcal{RN}(4) = \left[\left(\underline{Lim}(4)\right), \left(\overline{Lim}(4)\right)\right] == [3.5, 4.5]$$

$$\mathcal{RN}(5) = \left[\left(\underline{Lim}(5)\right), \left(\overline{Lim}(5)\right)\right] == [4, 5]$$

Applying Eqs (11) and (12):

$$\mathcal{R}\bar{\mathcal{N}}(x) = \left[x^{\ell} \quad x^{u}\right]$$

$$x^{\ell} = \frac{3+3.5+4}{3} = 3.5$$

$$x^{u} = \frac{4+4.5+5}{3} = 4.5$$

Hence, the rough interval of {3,4,5} is $\mathcal{R}\bar{\mathcal{N}}(x) = \left[x^{\ell} \quad x^{u}\right] = [3.5 \quad 4.5]$.

Similarly, the others can be calculated.

Table 4. Rough intervals of the experts' opinions.

Three experts		Specific capacitance	Potential window	Energy density	Power density	Stability	
						Capacitance retention	Cycles number
Specific capacitance		[1, 1]	[4.5, 5.5]	[1, 1]	[2, 2]	[2.1665, 2.61]	[2.1665, 2.61]
Potential window		[0.1852, 0.2268]	[1, 1]	[0.194, 0.2777]	[0.2283, 0.2949]	[0.5, 0.5]	[0.5, 0.5]
Energy density		[1, 1]	[3.8888, 5.3887]	[1, 1]	[2, 2]	[2.1665, 2.61]	[2.1665, 2.61]
Power density		[0.5, 0.5]	[3.5, 4.5]	[0.5, 0.5]	[1, 1]	[2, 2]	[2, 2]
Stability	Capacitance retention	[0.39797, 0.45355]	[2, 2]	[0.39797, 0.45355]	[0.5, 0.5]	[1, 1]	[1.1, 1.6]
	Cycles number	[0.39797, 0.45355]	[2, 2]	[0.39797, 0.45355]	[0.5, 0.5]	[0.69, 0.94]	[1, 1]

Finally, the steps of the rough-AHP are used to determine the interval weights of the criteria, as reported in Table 5. Moreover, we can get the crisp values using Eq (2). as also, Figure 2 illustrates the normalizing of the lower and upper interval weights of the criteria.

The obtained results show that the specific capacitance (SC) is the most significant, with a relative closeness value of (0.265592). This criterion (SC) denotes the amount of charge that could be stored in the energy storage devices, where the performance of supercapacitors is superb, with high values of SC. Consequently, this criterion is the most significant one. It is followed by energy density (ED) with a value of (0.264448). The ED is another significant factor in the electrochemical characteristics of the electrode materials. This criterion (ED) also is important in any supercapacitor to decide how long the supercapacitor can be utilized. The power density (PD) comes in the third rank with a value of (0.229159). This criterion (PD) is significant in determining how speedily an energy storage device can transfer energy.

In contrast, the capacitance retention (CR) was in the fourth rank with a value of (0.100845). The CR denotes cycling stability, which is considered an important factor for the evaluated performance of supercapacitors. It is followed by the cycle number (CN) with a value of (0.0.092616), which is strongly based on applying the appropriate energy storage device. Finally, the last significant criterion was the potential window (PW), with a value of (0.04734).

Table 5. Results of criteria weights using the Rough-AHP method.

Criteria	Rough weights	CN_i^{crisp}	Rank
Specific capacitance (SC)	[0.908896, 1]	0.265592	1
Potential window (PW)	[0.173596, 0.198927]	0.04734	6
Energy density (ED)	[0.88702, 0.996598]	0.264448	2
Power density (PD)	[0.7600112, 0.7625782]	0.229159	3
Capacitance retention (CR)	[0.363974, 0.404684]	0.100845	4
Cycles number (CN)	[0.336754, 0.370354]	0.092616	5

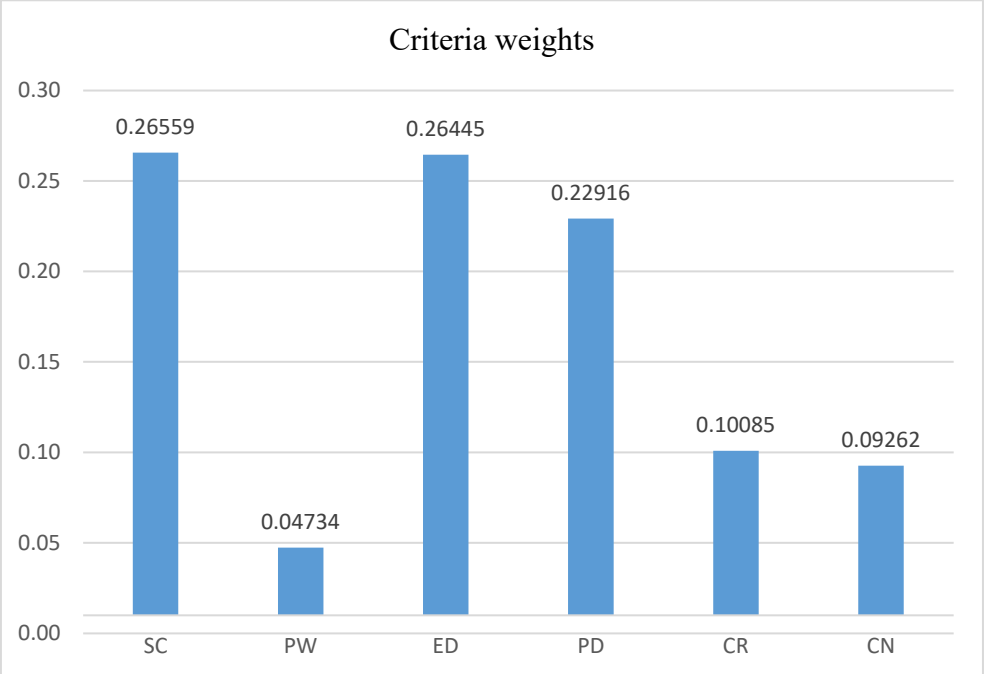

Figure 2. Results of criteria weights using Rough-AHP method.

Now, fourteen NEMs for HPSCs mentioned in the first column of Table 6 will be evaluated using rough EDAS and rough GRA methods, considering the rough weights of the criteria reported in Table 5.

Table 6 lists fourteen NEMs for HPSCs with their properties in the first column.

Table 6. Key interval properties of NEMs for HPSCs.

NEM		Specific capacitance ($F\ g^{-1}$)	Potential window (V)	Energy density ($Wh\ kg^{-1}$)	Power density ($W\ kg^{-1}$)	Stability		Ref.
						Capacitance retention	Cycles number	
		Δ	Δ	Δ	Δ	Δ	Δ	
Nanostructured carbon-based materials	Activated carbon materials (ACs)	100−300	2−2.7	142.4−308.3	0.7−7.6	70−91.4%	3000−30,000	[6,43−47]
	Carbon nanotubes (CNTs)	104−292	1−3	62.8−155.6	58.5−263.2	71−91%	1000−5000	[2,6,48,49]
	Graphene	120−483	1−1.3	26−28.5	8.1−25.1	89−90%	1200−10,000	[6−8]
Transition metal oxides/hydroxides-based materials	Ruthenium oxide (RuO_2)	407−720	0.8−1.4	17.6−30.9	4−14	80−92.7%	1000−10,000	[6,9,50,51]
	Manganese dioxide (MnO_2)	220−241	1−1.1	21.1−84.4	0.4−13.3	86.2−98.3%	1000−3000	[6,52,53]
	Nickel oxide (NiO)	1161−2018	0.4−2	22−132.3	0.5−1.65	92.4−99.7%	1000−5000	[6,54−59]
	Nickel hydroxide ($Ni(OH)_2$)	502−1868	0.5−0.6	35.78−56.5	0.11−0.5	81−97%	1000−10,000	[6,60−62]
	Vanadium pentoxide (V_2O_5)	343−1280	0.4−2	60.2−355	0.2−0.35	86.2−91%	5000−10,000	[6,63−65]
Conducting polymer-based material	Polyaniline (PANI)	300 - 950	0.7−1	15−100	0.2−28	60−88%	500−1000	[6,66,67]
	Polypyrrole (PPy)	52.5−2223	0.6−1.8	11.8−3.5	0.088−5.5	90−93%	2000−20,000	[33,68,69]
	Carbon–carbon composites (C-C)	201−261	3−3.7	62.8−123	58.5−255	94−129%	1000−10,000	[48,70]

Continued on next page

NEM		Specific capacitance ($F\ g^{-1}$)	Potential window (V)	Energy density ($Wh\ kg^{-1}$)	Power density ($W\ kg^{-1}$)	Stability		Ref.
						Capacitance retention	Cycles number	
		Δ	Δ	Δ	Δ	Δ	Δ	
Nanocomposite-based materials	Carbon-metal oxides composites (C-MOs)	313−1225	1.4−3	27.3−46.3	0.7−5.26	92.7−94%	2000−4000	[71−73]
	Carbon-conducting polymers composites (C-CPs)	432−1665	0.7−1	8.6−25	0.11−0.6	85−94%	1000−10,000	[74−77]
	Metal oxides-conducting polymers composites (MOs-CPs)	110−1625	0.7−1.5	12−20	0.075−3	83−94%	600−1000	[6,78,79]

In the first row, the key properties are mentioned, while in the second row, the type of the criterion is reported, where Δ denotes that the higher score is the best, and the criteria are of the benefit type. The first column in Table 6 denotes the main sections of NEMs, while the second column lists the fourteen NEMs for supercapacitors. In the third column, the range of the SCs for each nanostructured electrode material, which is the most significant criterion, is given. As seen, the best-nanostructured electrode material was the nickel oxide (NiO), with a range of (1161–2018 Fg^{-1}), while carbon nanotubes (CNTs) as electrode materials have the lowest SC, in the range of (104–292 Fg^{-1}). Potential window (PW) is given in the fourth column, where carbon-carbon composites (C-C) as electrode materials have the best value. The fifth column contains the energy density (ED) of each electrode material. In this criterion, the activated carbon materials (ACs) as electrodes have the best values, with the range of (142.4–308.3 $Wh\ kg^{-1}$), while metal oxides- conducting polymers composites (MOs-CPs) have the lowest values, in the range of (12–20 $Wh\ kg^{-1}$). The power density (PD) is given in the sixth column, and as seen, the best value was for carbon nanotubes (CNTs) as electrode materials. The seventh column was about capacitance retention (CR); in this criterion, the carbon-carbon composites (C-C) as electrode materials have the best value, while the Polyaniline (PANI) electrodes have the lowest values. The last column was for the cycle number (CN), and as seen, the activated carbon materials (ACs) have the best values, while metal oxides- conducting polymers composites (MOs-CPs) have the lowest values.

4.2. The results of the rough EDAS method

The rough EDAS method was used to evaluate the NEMs for HPSCs. Table 7 lists the values of $\mathcal{NE}_i^{\ell}$, $\mathcal{NE}_i^{u}$, their crisp values and their ranks. We can see clearly that the carbon–carbon composites (C-C), carbon nanotubes (CNTs) and activated carbon materials (ACs) have the highest averages of the $\mathcal{NE}_i^{\ell}$, $\mathcal{NE}_i^{u}$ values. This outcome was logical from the point of view of experts because these NEMs have outstanding SC, ED and PD, which are considered significant criteria for the evaluation of electrochemical properties in electrode materials for HPSCs. It can be observed that these NEMs contain carbon composites. Mostly, carbon materials are employed as electrodes for EDLCs because of their enhanced characteristics, such as great SSA [6,80]. Moreover, their thermal and electrochemical stability, great electrical conductivity, symmetrical galvanostatic charge-discharge profile and excellent rectangular form of cyclic voltammetry (CV) patterns suggest that carbon-based composites are suitable electrode materials [6,13,14]. The SC of the electrodes considerably depends on the SSA. Thus, due to the large SSA and the great porosity of the carbon composites, they have shown improved SC [6].

The four worst NEMs for HPSCs according to this method are metal oxides- conducting polymers composites (MOs-CPs), manganese dioxide (MnO_2), graphene and ruthenium oxide (RuO_2), with values of 0.120051478, 0.126482134, 0.160093041 and 0.177150806, respectively.

This result is due to these NEMs having low values of SC, ED and PD, which are considered significant criteria for evaluating the electrochemical properties of HPSCs. Although the metal oxides-conducting polymers composites (MOs-CPs) have relatively high values of SC, they have the lowest ED, PD and CN.

Table 7. Results of the NEMs for HPSCs ranking using the rough EDAS method.

NEM	$\mathcal{NE}_i^{\ell}$	$\mathcal{NE}_i^{u}$	Crisp	Rank
(ACs)	0.624068175	2.086882518	0.407192078	3
(CNTs)	0.796030073	3.042414414	0.573801877	2
Graphene	0.249227536	0.831835637	0.160093041	12
(RuO_2)	0.314617758	0.865008805	0.177150806	11
(MnO_2)	0.178543041	0.687774252	0.126482134	13
(NiO)	0.632393205	1.583489681	0.338186113	5
($Ni(OH)_2$)	0.417485046	1.322311386	0.260790126	6
(V_2O_5)	0.54000241	2.159702813	0.401453412	4
(PANI)	0.157371176	1.144262742	0.186473818	10
(PPy)	0.013676219	1.723085911	0.240373347	7
(C-C)	0.894406211	2.961716413	0.58115099	1
(C-MOs)	0.328984826	0.946056009	0.191241006	8
(C-CPs)	0.216115891	1.085094924	0.189322757	9
(MOs-CPs)	0.011612409	0.867781224	0.120051478	14

4.3. The results of the rough GRA method

In this subsection, the ranking of NEMs for HPSCs is reported using the rough GRA method.

Table 8 presents the values of $\mathcal{G}_{ij}^{\ell}$, $\mathcal{G}_{ij}^{u}$ and their crisp values that were obtained by Eq (2), with ranks.

The obtained ranks indicate that the best four nanostructured electrodes are vanadium pentoxide (V_2O_5), nickel oxide (NiO), carbon–carbon composites (C-C) and activated carbon materials (ACs), with values of 0.899804683, 0.780106205, 0.747478217 and 0.738646302, respectively.

Nanostructured TMOs, such as V_2O_5 and NiO, have been examined for use in energy storage systems (supercapacitors and lithium-ion batteries) owing to their high SC, ED and PD [81−83]. V_2O_5 has a specific interest owing to layered structures and well-known inserting ions between the layers. Thus, it can be employed as electrodes in electrochemical applications, such as batteries or supercapacitors [84]. NiO is particularly attractive due to its high theoretical capacitance of 2573 Fg^{-1}, good thermal stability and chemical stability. Because of rapid redox reactions, reduced diffusion tracks and great SCA in the solid phase, nano/micro-materials have wide applications in supercapacitors [26]. In addition, the mesoporous NiO exhibited a better rate capability, which is because the well-ordered mesopores do not limit the movement of the ions within the pores [26].

The four worst NEMs for HPSCs according to this method are polyaniline (PANI), metal oxides-conducting polymers composites (MOs-CPs), manganese dioxide (MnO_2) and ruthenium oxide (RuO_2), with values of 0.002363447, 0.056136119, 0.107041622 and 0.126913722, respectively. This result is due to these NEMs having low SC, ED and PD values, as explained above.

Table 8. Results of the NEMs for HPSCs ranking using the rough GRA method.

NEM	$\mathcal{G}_{ij}^{\ell}$	$\mathcal{G}_{ij}^{u}$	Crisp	Rank
(ACs)	0.096066541	0.089486958	0.738646302	4
(CNTs)	0.084254985	0.083437437	0.565028425	5
Graphene	0.066221478	0.059496494	0.13427894	10
(RuO_2)	0.06537249	0.061402026	0.126913722	11
(MnO_2)	0.064541698	0.059802633	0.107041622	12
(NiO)	0.101923334	0.089292469	0.780106205	2
($Ni(OH)_2$)	0.06889424	0.080664301	0.309353299	7
(V_2O_5)	0.079427377	0.10261155	0.899804683	1
(PANI)	0.059347887	0.065366471	0.002363447	14
(PPy)	0.064273424	0.096463052	0.470863831	6
(C-C)	0.095099067	0.090490914	0.747478217	3
(C-MOs)	0.071188845	0.067001979	0.249040575	8
(C-CPs)	0.06609203	0.073975384	0.193785124	9
(MOs-CPs)	0.060743217	0.071951396	0.056136119	13

4.4. Comparative analysis

In this subsection, the obtained ranks using the R-EDAS and R-GRA are compared to investigate the relationship between the obtained ranks of the NEMs for HPSCs. Table 9 lists the obtained ranks by both methods.

We can readily see from Table 9 that the best five NEMs using both methods are vanadium pentoxide (V2O5), nickel oxide (NiO), carbon–carbon composites (C-C) activated carbon materials

(ACs) and carbon nanotubes (CNTs), with slight differences in ranks due to the different methodologies of each method.

Similarly, it can be noted that the worst five substances are metal oxides- conducting polymers composites (MOs-CPs), manganese dioxide (MnO2), graphene, ruthenium oxide (RuO2) and polyaniline (PANI).

Table 9. Results of the comparison between R-EDAS and R-GRA methods.

NEM	R-EDAS	R-GRA
(ACs)	3	4
(CNTs)	2	5
Graphene	12	10
(RuO_2)	11	11
(MnO_2)	13	12
(NiO)	5	2
($Ni(OH)_2$)	6	7
(V_2O_5)	4	1
(PANI)	10	14
(PPy)	7	6
(C-C)	1	3
(C-MOs)	8	8
(C-CPs)	9	9
(MOs-CPs)	14	13

In addition, Figure 3 illustrates the comparative rankings of the NEMs for HPSCs.

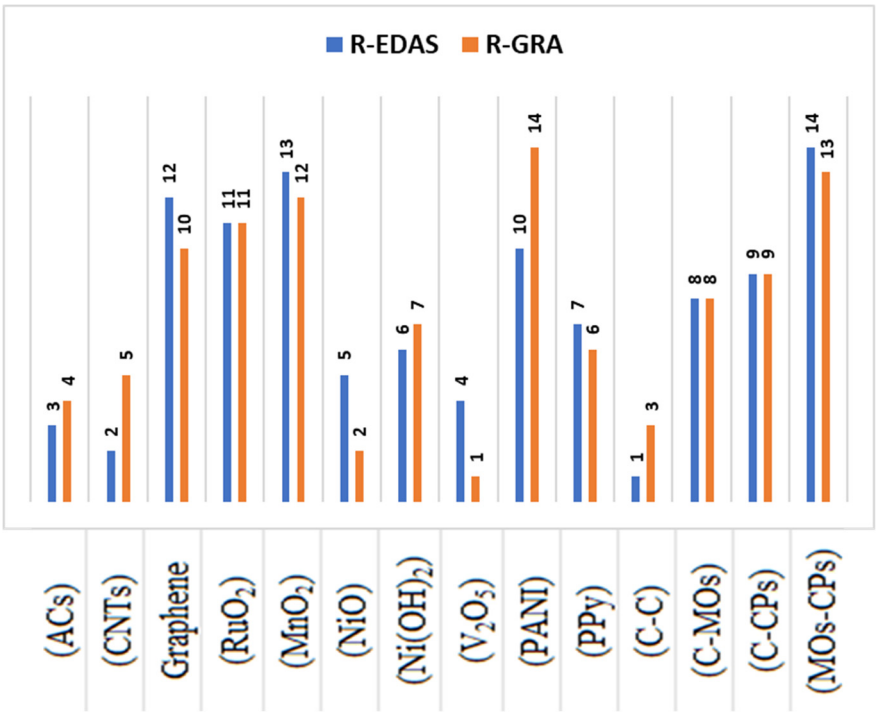

Figure 3. Graphical illustration of the comparison between R-EDAS and R-GRA methods.

The Pearson correlation coefficient between the obtained ranks by both methods is equal to 0.877, emphasizing the positive relationship between the obtained ranks; and the p-value of 0.0000383, which was a minimal value, confirmed the stability of the positive relationship between the ranks. Figure 4 illustrates the preference ranking using both methods.

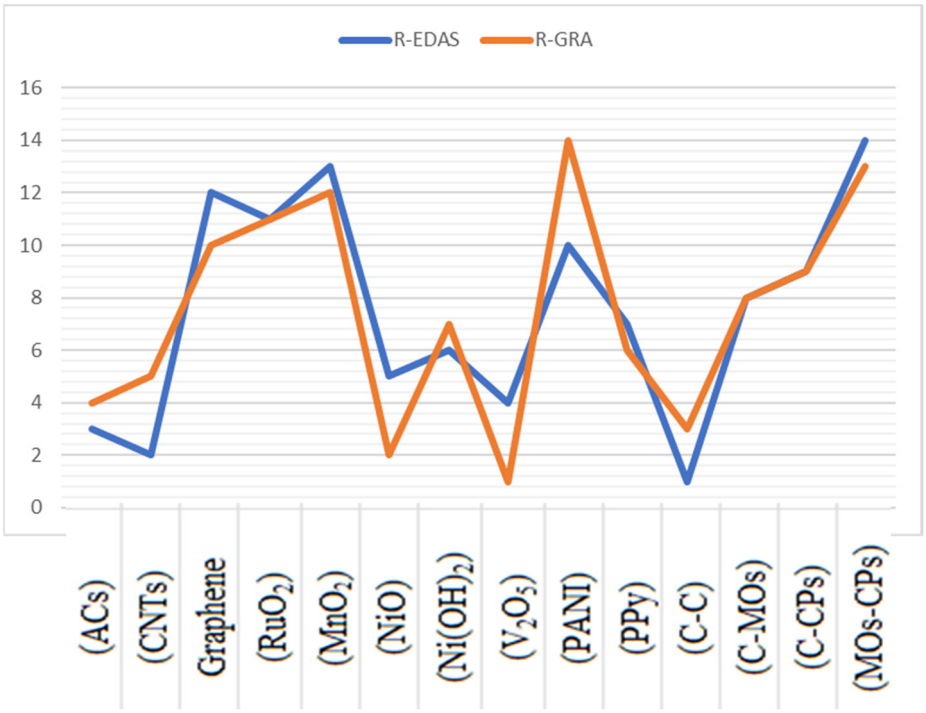

Figure 4. Comparison of preference rankings of the NEMs for HPSCs with R-EDAS and R-GRA methods.

We can deduce the possibility of employing a rough-MCDM approach in evaluating the NEMs for HPSCs and get a logical evaluation that is useful to support DM in this kind of problem.

5. Conclusions

This work develops an approach to evaluate and rank NEMs for HPSCs based on the vague values of the electrochemical properties. To flexibly facilitate the group decision-making, the proposed approach combines the AHP method and the rough numbers to determine the weight of the criteria. Similarly, to flexibly manipulate the vagueness values of the electrochemical properties without pre-assumptions or any extra auxiliary information, the proposed approach integrates the advantages of the R-AHP method and the advantages of the R-EDAS/R-GRA methods to rank the NEMs. The results indicate that the most important criteria and electrochemical properties were specific capacitance, energy density and power density. In addition, the compromise results indicated that vanadium pentoxide (V_2O_5), nickel oxide (NiO), carbon–carbon composites (C-C), activated carbon materials (ACs) and carbon nanotubes (CNTs) are the five best NEMs for HPSCs. Meanwhile, the last five ranks of NEMs are metal oxides- conducting polymers composites (MOs-CPs), manganese dioxide (MnO_2), graphene, ruthenium oxide (RuO_2) and polyaniline (PANI). This work can be extended to include the different types of uncertainty for future works.

Authors' contributions

Ibrahim M. Hezam: Conceptualization, Formal analysis, Funding acquisition, Investigation, Methodology, Project administration, Resources, Software, Validation, Visualization, Writing - original draft, Writing - review editing. Aref M Al-Syadi: Data collection and curation, Writing parts of the physics background, discussion of the related results, review editing. Abdelaziz Foul: Revision of draft preparation. Ahmad Alshamrani and Jeonghwan Gwak: Revision of draft preparation. All authors read and approved the final manuscript.

Funding

The authors extend their appreciation to the Deputyship for Research & Innovation, Ministry of Education in Saudi Arabia for funding this research work through the project no. (IFKSURG-2-1752).

Acknowledgments

We should like to thank the Editors of the journal as well as the anonymous reviewers for their valuable suggestions that make the paper stronger and more consistent.

Conflict of interest

We have no conflicts with competing interests to disclose.

References

1. C. Zhao, W. Zheng, A review for aqueous electrochemical supercapacitors, *Front. Energy Res.*, **3** (2015). https://doi.org/10.3389/fenrg.2015.00023
2. L. Lai, H. Yang, L. Wang, B. K. Teh, J. Zhong, H. Chou, et al., Preparation of supercapacitor electrodes through selection of graphene surface functionalities, *ACS Nano*, **6** (2012), 5941–5951. https://doi.org/10.1021/nn3008096
3. E. Frackowiak, Carbon materials for supercapacitor application, *Phys. Chem. Chem. Phys.*, **9** (2007), 1774. https://doi.org/10.1039/b618139m
4. M. Inagaki, H. Konno, O. Tanaike, Carbon materials for electrochemical capacitors, *J. Power Sources*, **195** (2010), 7880–7903. https://doi.org/10.1016/j.jpowsour.2010.06.036
5. Z. S. Wu, W. Ren, D. W. Wang, F. Li, B. Liu, H. M. Cheng, High-energy MnO_2 nanowire/graphene and graphene asymmetric electrochemical capacitors, *ACS Nano*, **4** (2010), 5835–5842. https://doi.org/10.1021/nn101754k
6. P. Forouzandeh, V. Kumaravel, S. C. Pillai, Electrode materials for supercapacitors: a review of recent advances, *Catalysts*, **10** (2020), 969. https://doi.org/10.3390/catal10090969
7. Y. Wang, Z. Shi, Y. Huang, Y. Ma, C. Wang, M. Chen, et al., Supercapacitor devices based on graphene materials, *J. Phys. Chem. C*, **113** (2009), 13103–13107. https://doi.org/10.1021/jp902214f

8. Y. Shabangoli, M. S. Rahmanifar, A. Noori, M. F. El-Kady, R. B. Kaner, M. F. Mousavi, Nile blue functionalized graphene aerogel as a pseudocapacitive negative electrode material across the full pH range, *ACS Nano*, **13** (2019), 12567–12576. https://doi.org/10.1021/acsnano.9b03351
9. H. Ma, D. Kong, Y. Xu, X. Xie, Y. Tao, Z. Xiao, et al., Disassembly-reassembly approach to RuO_2/graphene composites for ultrahigh volumetric capacitance supercapacitor, *Small*, **13** (2017), 1701026. https://doi.org/10.1002/smll.201701026
10. N. Syarif, T. A. Ivandini, W. Wibowo, Direct synthesis carbon/metal oxide composites for electrochemical capacitors electrode, *Int. Trans. J. Eng. Manage. Appl. Sci. Technol.*, **3** (2012), 21–34. Available from: https://tuengr.com/V03/21-34.pdf.
11. L. L. Zhang, X. S. Zhao, Carbon-based materials as supercapacitor electrodes, *Chem. Soc. Rev.*, **38** (2009), 2520–2531. https://doi.org/10.1039/b813846j
12. E. Frackowiak, F. Béguin, Carbon materials for the electrochemical storage of energy in capacitors, *Carbon*, **39** (2001), 937–950. https://doi.org/10.1016/S0008-6223(00)00183-4
13. P. Simon, A. Burke, Nanostructured carbons: double-layer capacitance and more, *Electrochem. Soc. Interface*, **17** (2008), 38–43. https://doi.org/10.1149/2.F05081IF
14. E. Frackowiak, K. Metenier, V. Bertagna, F. Beguin, Supercapacitor electrodes from multiwalled carbon nanotubes, *Appl. Phys. Lett.*, **77** (2000), 2421–2423. https://doi.org/10.1063/1.1290146
15. M. Pumera, Graphene-based nanomaterials and their electrochemistry, *Chem. Soc. Rev.*, **39** (2010), 4146–4157. https://doi.org/10.1039/c002690p
16. Y. B. Tan, J. M. Lee, Graphene for supercapacitor applications, *J. Mater. Chem. A*, **1** (2013), 14814–14843. https://doi.org/10.1039/c3ta12193c
17. T. Y. Kim, G. Jung, S. Yoo, K. S. Suh, R. S. Ruoff, Activated graphene-based carbons as supercapacitor electrodes with macro- and mesopores, *ACS Nano*, **7** (2013), 6899–6905. https://doi.org/10.1021/nn402077v
18. V. C. Lokhande, A. C. Lokhande, C. D. Lokhande, J. H. Kim, T. Ji, Supercapacitive composite metal oxide electrodes formed with carbon, metal oxides and conducting polymers, *J Alloys Compd.*, **682** (2016), 381–403. https://doi.org/10.1016/j.jallcom.2016.04.242
19. J. Y. Hwang, M. F. El-Kady, Y. Wang, L. Wang, Y. Shao, K. Marsh, et al., Direct preparation and processing of graphene/RuO_2 nanocomposite electrodes for high-performance capacitive energy storage, *Nano Energy*, **18** (2015), 57–70. https://doi.org/10.1016/j.nanoen.2015.09.009
20. D. Zhao, X. Guo, Y. Gao, F. Gao, An electrochemical capacitor electrode based on porous carbon spheres hybrided with polyaniline and nanoscale ruthenium oxide, *ACS Appl. Mater. Interfaces*, **4** (2012), 5583–5589. https://doi.org/10.1021/am301484s
21. I. Acznik, K. Lota, A. Sierczynska, G. Lota, Carbon-supported manganese dioxide as electrode material for asymmetric electrochemical capacitors, *Int. J. Electrochem. Sci.*, **9** (2014), 2518–2534. Available from: http://www.electrochemsci.org/papers/vol9/90502518.pdf.
22. S. Chen, J. Zhu, X. Wu, Q. Han, X. Wang, Graphene oxide-MnO_2 nanocomposites for supercapacitors, *ACS Nano*, **4** (2010), 2822–2830. https://doi.org/10.1021/nn901311t
23. J. G. Wang, F. Kang, B. Wei, Engineering of MnO_2-based nanocomposites for high-performance supercapacitors, *Prog. Mater. Sci.*, **74** (2015), 51–124. https://doi.org/10.1016/j.pmatsci.2015.04.003
24. D. D. Zhao, M. W. Xu, W. J. Zhou, J. Zhang, H. L. Li, Preparation of ordered mesoporous nickel oxide film electrodes via lyotropic liquid crystal templated electrodeposition route, *Electrochim. Acta*, **53** (2008), 2699–2705. https://doi.org/10.1016/j.electacta.2007.07.053

25. Y. Wang, Y. Xia, Electrochemical capacitance characterization of NiO with ordered mesoporous structure synthesized by template SBA-15, *Electrochim. Acta*, **51** (2006), 3223–3227. https://doi.org/10.1016/j.electacta.2005.09.013
26. B. Li, M. Zheng, H. Xue, H. Pang, High performance electrochemical capacitor materials focusing on nickel based materials, *Inorg. Chem. Front.*, **3** (2016), 175–202. https://doi.org/10.1039/C5QI00187K
27. S. R. Ede, S. Anantharaj, K. T. Kumaran, S. Mishrab, S. Kundu, One step synthesis of Ni/$Ni(OH)_2$ nano sheets (NSs) and their application in asymmetric supercapacitors, *RSC Adv.*, **7** (2017), 5898–5911. https://doi.org/10.1039/C6RA26584G
28. H. Wang, H. S. Casalongue, Y. Liang, H. Dai, $Ni(OH)_2$ nanoplates grown on graphene as advanced electrochemical pseudocapacitor materials, *J. Am. Chem. Soc.*, **132** (2010), 7472–7477. https://doi.org/10.1021/ja102267j
29. Q. T. Qu, L. L. Liu, Y. P. Wu, R. Holze, Electrochemical behavior of $V_2O_5{\cdot}0.6H_2O$ nanoribbons in neutral aqueous electrolyte solution, *Electrochim. Acta*, **96** (2013), 8–12. https://doi.org/10.1016/j.electacta.2013.02.078
30. V. Augustyn, P. Simon, B. Dunn, Pseudocapacitive oxide materials for high-rate electrochemical energy storage, *Energy Environ. Sci.*, **7** (2014), 1597. https://doi.org/10.1039/c3ee44164d
31. Y. Liu, J. Zhou, J. Tang, W. Tang, Three-dimensional, chemically bonded polypyrrole/bacterial cellulose/graphene composites for high-performance supercapacitors, *Chem. Mater.*, **27** (2015), 7034–7041. https://doi.org/10.1021/acs.chemmater.5b03060
32. G. A. Snook, P. Kao, A. S. Best, Conducting-polymer-based supercapacitor devices and electrodes, *J. Power Sources*, **196** (2011), 1–12. https://doi.org/10.1016/j.jpowsour.2010.06.084
33. C. Zhou, Y. Zhang, Y. Li, J. Liu, Construction of high-capacitance 3D CoO@Polypyrrole nanowire array electrode for aqueous asymmetric supercapacitor, *Nano Lett.*, **13** (2013), 2078–2085. https://doi.org/10.1021/nl400378j
34. Poonam, K. Sharma, A. Arora, S. K. Tripathi, Review of supercapacitors: materials and devices, *J. Energy Storage*, **21** (2019), 801–825. https://doi.org/10.1016/j.est.2019.01.010
35. M. Mastragostino, Conducting polymers as electrode materials in supercapacitors, *Solid State Ionics*, **148** (2002), 493–498. https://doi.org/10.1016/S0167-2738(02)00093-0
36. K. Xie, B. Wei, Materials and structures for stretchable energy storage and conversion devices, *Adv. Mater.*, **26** (2014), 3592–3617. https://doi.org/10.1002/adma.201305919
37. I. I. Karayalcin, The analytic hierarchy process: planning, priority setting, resource allocation, *Eur. J. Oper. Res.*, **9** (1982), 97–98. https://doi.org/10.1016/0377-2217(82)90022-4
38. Z. Pawlak, Rough sets, *Int. J. Comput. Inf. Sci.*, **11** (1982), 341–356. https://doi.org/10.1007/BF01001956
39. T. L. Saaty, *The Analytic Hierarchy Process: Planning, Priority Setting, Resource Allocation (Decision Making Series)*, McGraw-Hill, (1980), 1–287.
40. M. K. Ghorabaee, E. K. Zavadskas, L. Olfat, Z. Turskis, Multi-criteria inventory classification using a new method of evaluation based on distance from average solution (EDAS), *Informatica*, **26** (2015), 435–451. https://doi.org/10.15388/Informatica.2015.57
41. J. L. Deng, Introduction to Grey system theory, *J. Grey Syst.*, **1** (1989), 1–24.
42. T. C. Chang, S. J. Lin, Grey relation analysis of carbon dioxide emissions from industrial production and energy uses in Taiwan, *J. Environ. Manage.*, **56** (1999), 247–257. https://doi.org/10.1006/jema.1999.0288

43. L. Li, X. Wang, S. Wang, Z. Cao, Z. Wu, H. Wang, et al., Activated carbon prepared from lignite as supercapacitor electrode materials, *Electroanalysis*, **28** (2016), 243–248. https://doi.org/10.1002/elan.201500532
44. M. Zhang, J. Cheng, L. Zhang, Y. Li, M. S. Chen, Y. Chen, et al., Activated carbon by one-step calcination of deoxygenated agar for high voltage lithium ion supercapacitor, *ACS Sustain. Chem. Eng.*, **8** (2020), 3637–3643. https://doi.org/10.1021/acssuschemeng.9b06347
45. F. Cheng, X. Yang, S. Zhang, W. Lu, Boosting the supercapacitor performances of activated carbon with carbon nanomaterials, *J. Power Sources*, **450** (2020), 227678. https://doi.org/10.1016/j.jpowsour.2019.227678
46. Y. J. Hsiao, L. Y. Lin, Efficient pore engineering in carbonized zeolitic imidazolate Framework-8 via chemical and physical methods as active materials for supercapacitors, *J. Power Sources*, **486** (2021), 229370. https://doi.org/10.1016/j.jpowsour.2020.229370
47. Y. H. Chiu, L. Y. Lin, Effect of activating agents for producing activated carbon using a facile one-step synthesis with waste coffee grounds for symmetric supercapacitors, *J. Taiwan Inst. Chem. Eng.*, **101** (2019), 177–185. https://doi.org/10.1016/j.jtice.2019.04.050
48. Q. Cheng, J. Tang, J. Ma, H. Zhang, N. Shinyaa, L. C. Qin, Graphene and carbon nanotube composite electrodes for supercapacitors with ultra-high energy density, *Phys. Chem. Chem. Phys.*, **13** (2011), 17615. https://doi.org/10.1039/c1cp21910c
49. Q. Liu, J. Yang, X. Luo, Y. Miao, Y. Zhang, W. Xu, et al., Fabrication of a fibrous MnO_2@MXene/CNT electrode for high-performance flexible supercapacitor, *Ceram. Int.*, **46** (2020), 11874–11881. https://doi.org/10.1016/j.ceramint.2020.01.222
50. H. Kim, B. N. Popov, Characterization of hydrous ruthenium oxide/carbon nanocomposite supercapacitors prepared by a colloidal method, *J. Power Sources*, **104** (2002), 52–61. https://doi.org/10.1016/S0378-7753(01)00903-X
51. S. Kong, K. Cheng, T. Ouyang, Y. Gao, K. Ye, G. Wang, et al., Facile electrodepositing processed of RuO_2-graphene nanosheets-CNT composites as a binder-free electrode for electrochemical supercapacitors, *Electrochim. Acta*, **246** (2017), 433–442. https://doi.org/10.1016/j.electacta.2017.06.019
52. O. Ghodbane, J. L. Pascal, F. Favier, Microstructural effects on charge-storage properties in MnO_2-based electrochemical supercapacitors, *ACS Appl. Mater. Interfaces*, **1** (2009), 1130–1139. https://doi.org/10.1021/am900094e
53. J. Dong, G. Lu, F. Wu, C. Xu, X. Kang, Z. Cheng, Facile synthesis of a nitrogen-doped graphene flower-like MnO_2 nanocomposite and its application in supercapacitors, *Appl. Surf. Sci.*, **427** (2018), 986–993. https://doi.org/10.1016/j.apsusc.2017.07.291
54. Z. Lu, Z. Chang, J. Liu, X. Sun, Stable ultrahigh specific capacitance of NiO nanorod arrays, *Nano Res.*, **4** (2011), 658–665. https://doi.org/10.1007/s12274-011-0121-1
55. P. Liu, M. Yang, S. Zhou, Y. Huang, Y. Zhu, Hierarchical shell-core structures of concave spherical NiO nanospines@carbon for high performance supercapacitor electrodes, *Electrochim. Acta*, **294** (2019), 383–390. https://doi.org/10.1016/j.electacta.2018.10.112
56. C. S. Kwak, T. H. Ko, J. H. Lee, H. Y. Kim, B. S. Kim, Flexible transparent symmetric solid-state supercapacitors based on NiO-decorated nanofiber-based composite electrodes with excellent mechanical flexibility and cyclability, *ACS Appl. Energy Mater.*, **3** (2020), 2394–2403. https://doi.org/10.1021/acsaem.9b02073

57. A. Ray, A. Roy, S. Saha, M. Ghosh, S. R. Chowdhury, T. Maiyalagan, et al., Electrochemical energy storage properties of Ni-Mn-Oxide electrodes for advance asymmetric supercapacitor application, *Langmuir*, **35** (2019), 8257–8267. https://doi.org/10.1021/acs.langmuir.9b00955
58. P. Y. Lee, L. Y. Lin, Developing zeolitic imidazolate frameworks 67-derived fluorides using 2-methylimidazole and ammonia fluoride for energy storage and electrocatalysis, *Energy*, **239** (2022), 122129. https://doi.org/10.1016/j.energy.2021.122129
59. K. L. Chiu, L. Y. Lin, Applied potential-dependent performance of the nickel cobalt oxysulfide nanotube/nickel molybdenum oxide nanosheet core–shell structure in energy storage and oxygen evolution, *J. Mater. Chem. A*, **7** (2019), 4626–4639. https://doi.org/10.1039/C8TA11471D
60. H. B. Li, M. H. Yu, F. X. Wang, P. Liu, Y. Liang, J. Xiao, et al., Amorphous nickel hydroxide nanospheres with ultrahigh capacitance and energy density as electrochemical pseudocapacitor materials, *Nat. Commun.*, **4** (2013), 1894. https://doi.org/10.1038/ncomms2932
61. Z. Xiao, P. Liu, J. Zhang, H. Qi, J. Liu, B. Li, et al., Pillar-coordinated strategy to modulate phase transfer of α-$Ni(OH)_2$ for enhanced supercapacitor application, *ACS Appl. Energy Mater.*, **3** (2020), 5628–5636. https://doi.org/10.1021/acsaem.0c00596
62. T. Xia, X. Zhang, J. Zhao, Q. Li, C. Ao, R. Hu, et al., Flexible and conductive carbonized cotton fabrics coupled with a nanostructured $Ni(OH)_2$ coating for high performance aqueous symmetric supercapacitors, *ACS Sustainable Chem. Eng.*, **7** (2019), 5231–5239. https://doi.org/10.1021/acssuschemeng.8b06150
63. M. J. Deng, L. H. Yeh, Y. H. Lin, J. M. Chen, T. H. Chou, 3D network V_2O_5 electrodes in a gel electrolyte for high-voltage wearable symmetric pseudocapacitors, *ACS Appl. Mater. Interfaces*, **11** (2019), 29838–29848. https://doi.org/10.1021/acsami.9b07845
64. H. C. Chen, Y. C. Lin, Y. L. Chen, C. J. Chen, Facile fabrication of three-dimensional hierarchical nanoarchitectures of VO_2/Graphene@NiS_2 hybrid aerogel for high-performance all-solid-state asymmetric supercapacitors with ultrahigh energy density, *ACS Appl. Energy Mater.*, **2** (2019), 459–467. https://doi.org/10.1021/acsaem.8b01486
65. W. Bi, Y. Wu, C. Liu, J. Wang, Y. Du, G. Gao, et al., Gradient oxygen vacancies in V_2O_5/PEDOT nanocables for high-performance supercapacitors, *ACS Appl. Energy Mater.*, **2** (2019), 668–677. https://doi.org/10.1021/acsaem.8b01676
66. K. Wang, J. Huang, Z. Wei, Conducting polyaniline nanowire arrays for high performance supercapacitors, *J. Phys. Chem. C*, **114** (2010), 8062–8067. https://doi.org/10.1021/jp9113255
67. C. C. Hu, K. H. Chang, M. C. Lin, Y. T. Wu, Design and tailoring of the nanotubular arrayed architecture of hydrous RuO_2 for next generation supercapacitors, *Nano Lett.*, **6** (2006), 2690–2695. https://doi.org/10.1021/nl061576a
68. Y. Shi, L. Pan, B. Liu, Y. Wang, Y. Cui, Z. Bao, et al., Nanostructured conductive polypyrrole hydrogels as high-performance, flexible supercapacitor electrodes, *J. Mater. Chem. A*, **2** (2014), 6086–6091. https://doi.org/10.1039/C4TA00484A
69. P. Bober, N. Gavrilov, A. Kovalcik, M. Mičušík, C. Unterweger, I. A. Pašti, et al., Electrochemical properties of lignin/polypyrrole composites and their carbonized analogues, *Mater. Chem. Phys.*, **213** (2018), 352–361. https://doi.org/10.1016/j.matchemphys.2018.04.043
70. F. Zhang, J. Tang, N. Shinya, L. C. Qin, Hybrid graphene electrodes for supercapacitors of high energy density, *Chem. Phys. Lett.*, **584** (2013), 124–129. https://doi.org/10.1016/j.cplett.2013.08.021

71. H. Wang, H. Yi, X. Chen, X. Wang, Asymmetric supercapacitors based on nano-architectured nickel oxide/graphene foam and hierarchical porous nitrogen-doped carbon nanotubes with ultrahigh-rate performance, *J. Mater. Chem. A*, **2** (2014), 3223–3230. https://doi.org/10.1039/C3TA15046A
72. S. D. Perera, B. Patel, N. Nijem, K. Roodenko, O. Seitz, J. P. Ferraris, et al., Vanadium oxide nanowire-carbon nanotube binder-free flexible electrodes for supercapacitors, *Adv. Energy Mater.*, **1** (2011), 936–945. https://doi.org/10.1002/aenm.201100221
73. L. Hu, N. Yan, Q. Chen, P. Zhang, H. Zhong, X. Zheng, et al., Fabrication based on the kirkendall effect of Co_3O_4 porous nanocages with extraordinarily high capacity for lithium storage, *Chem. - A Eur. J.*, **18** (2012), 8971–8977. https://doi.org/10.1002/chem.201200770
74. Y. Yang, Y. Xi, J. Li, G. Wei, N. I. Klyui, W. Han, Flexible supercapacitors based on polyaniline arrays coated graphene aerogel electrodes, *Nanoscale Res. Lett.*, **12** (2017), 394. https://doi.org/10.1186/s11671-017-2159-9
75. J. Yan, T. Wei, Z. Fan, W. Qian, M. Zhang, X. Shen, et al., Preparation of graphene nanosheet/carbon nanotube/polyaniline composite as electrode material for supercapacitors, *J. Power Sources*, **195** (2010), 3041–3045. https://doi.org/10.1016/j.jpowsour.2009.11.028
76. J. Jaidev, S. Ramaprabhu, Poly(p-phenylenediamine)/graphene nanocomposites for supercapacitor applications, *J. Mater. Chem.*, **22** (2012), 18775–18783. https://doi.org/10.1039/C2JM33627H
77. M. S. Nam, U. Patil, B. Park, H. B. Sim, S. C. Jun, A binder free synthesis of 1D PANI and 2D MoS_2 nanostructured hybrid composite electrodes by the electrophoretic deposition (EPD) method for supercapacitor application, *RSC Adv.*, **6** (2016), 101592–101601. https://doi.org/10.1039/C6RA16078F
78. Y. Liu, B. Zhang, Y. Yang, Z. Chang, Z. Wen, Y. Wu, Polypyrrole-coated α-MoO_3 nanobelts with good electrochemical performance as anode materials for aqueous supercapacitors, *J. Mater. Chem. A*, **1** (2013), 13582. https://doi.org/10.1039/c3ta12902k
79. R. P. Raj, P. Ragupathy, S. Mohan, Remarkable capacitive behavior of a Co_3O_4–polyindole composite as electrode material for supercapacitor applications, *J. Mater. Chem. A*, **3** (2015), 24338–24348. https://doi.org/10.1039/C5TA07046E
80. Z. S. Iro, C. Subramani, S. S. Dash, A brief review on electrode materials for supercapacitor, *Int. J. Electrochem. Sci.*, **11** (2016), 10628–10643. https://doi.org/10.20964/2016.12.50
81. A. M. Al-Syadi, Electrochemical performance of Na_2O–Li_2O–P_2S_5–V_2S_5 glass–ceramic nanocomposites as electrodes for supercapacitors, *Appl. Phys. A*, **127** (2021), 755. https://doi.org/10.1007/s00339-021-04899-7
82. A. M. Al-Syadi, M. S. Al-Assiri, H. M. A. Hassan, G. E. Enany, M. M. El-Desoky, Effect of sulfur addition on the electrochemical performance of lithium-vanadium-phosphate glasses as electrodes for energy storage devices, *J. Electroanal. Chem.*, **804** (2017), 36–41. https://doi.org/10.1016/j.jelechem.2017.09.041
83. M. M. El-Desoky, A. M. Al-Syadi, M. S. Al-Assiri, H. M. A. Hassan, G. E. Enany, Electrochemical performance of novel $Li_3V_2(PO_4)_3$ glass-ceramic nanocomposites as electrodes for energy storage devices, *J. Solid State Electrochem.*, **20** (2016), 2663–2671. https://doi.org/10.1007/s10008-016-3267-7

84. M. M. El-Desoky, A. M. Al-Syadi, M. S. Al-Assiri, H. M. A. Hassan, Effect of sulfur addition and nanocrystallization on the transport properties of lithium–vanadium–phosphate glasses, *J. Mater. Sci. Mater. Electron.*, **29** (2018), 968–977. https://doi.org/10.1007/s10854-017-7994-z

Appendix

Table A1. Abbreviations and acronyms.

RS	Rough set
RN	Rough number
DM(s)	Decision maker(s)
MCDM	Multiple criteria decision making
R-AHP	Rough analytic hierarchy process
R-EDAS	Rough evaluation based on distance from average solution
SC	Specific capacitance
PW	Potential window
ED	Energy density
PD	Power density
CR	Capacitance retention
CN	Cycles number
SSA	Specific surface area
NEMs	Nanostructured electrode materials
HPSCs	High-performance supercapacitors

AIMS Press